Atomic-binding-energy oscillations

Berthold-Georg Englert and Julian Schwinger
Department of Physics, University of California, Los Angeles, California 90024
(Received 28 January 1985)

We investigate the oscillatory supplement to the statistical nonrelativistic binding-energy formula for neutral atoms. The semiclassical approach proves capable of deriving these oscillations. It turns out that their amplitude is proportional to $Z^{4/3}$ (Z is the number of electrons), and that their period is determined by the maximum angular momentum available in Thomas-Fermi atoms, i.e., $0.928Z^{1/3}$. Our calculation also provides an understanding of the peculiar shape of the oscillations, which show sharp minima and wide, structured maxima.

INTRODUCTION

The Thomas-Fermi (TF) statistical model of the atom, together with its quantal refinements, is known to produce this remarkably simple formula[1–3]

$$-E_{\text{stat}}=0.768\,745Z^{7/3}-\tfrac{1}{2}Z^2+0.269\,900Z^{5/3} \qquad (1)$$

for the electronic binding energy of a neutral atom with Z electrons. The relative difference between E_{stat} and Hartree-Fock (HF) results[4] E_{HF} is less than one-fifth of a percent for $Z\geq 22$ and less than one-tenth of a percent for $Z\geq 56$. This is illustrated in Fig. 1, where one also observes that the deviation is oscillatory with a period that increases slowly with Z. A plot of the absolute difference between the HF binding energy and the statistical one, presented in Fig. 2, shows the surprisingly high regularity of these oscillations.[5] They possess an amplitude proportional to $Z^{4/3}$, as would be natural for the leading correction to E_{stat} of (1), and are periodic in $Z^{1/3}$. A particularly interesting property of these atomic-binding-energy oscillations is the sharp, structureless minima in contrast to the broad maxima with their evolving double-peak structure.

The purpose of the present paper is to derive these oscillations by further improvement of the statistical method.[6] The basic idea is to incorporate semiclassical quantization in order to include more of the individuality of the electrons. The general scheme has been developed in a preceding paper[7] and has been applied to the circumstance of linear degeneracy in another one.[8] We shall make use of the terminology and notation introduced there, referring to these papers as I and II, respectively.

There is a common reaction that these oscillations have something to do with the filling of atomic shells. But this

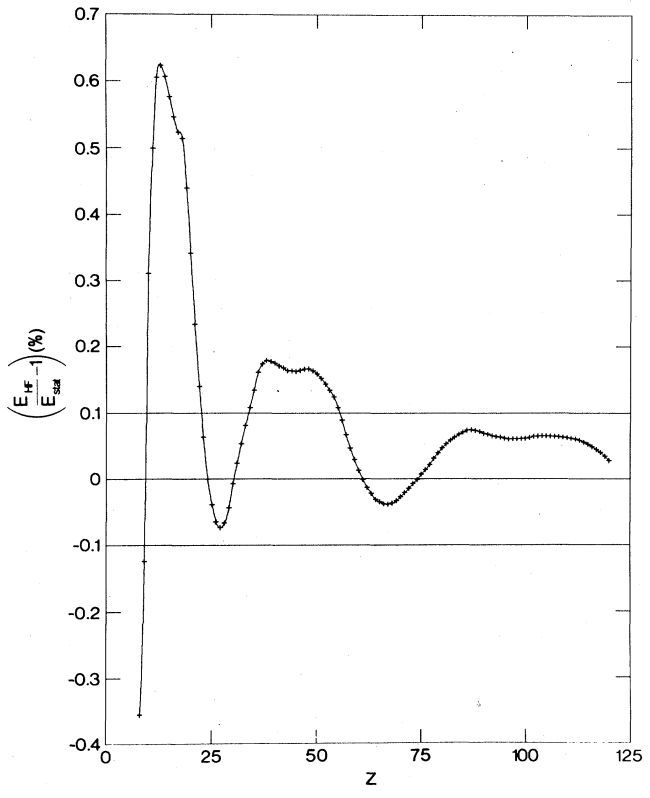

FIG. 1. Relative deviation, in %, between HF binding energies and the statistical formula (1), as a function of Z.

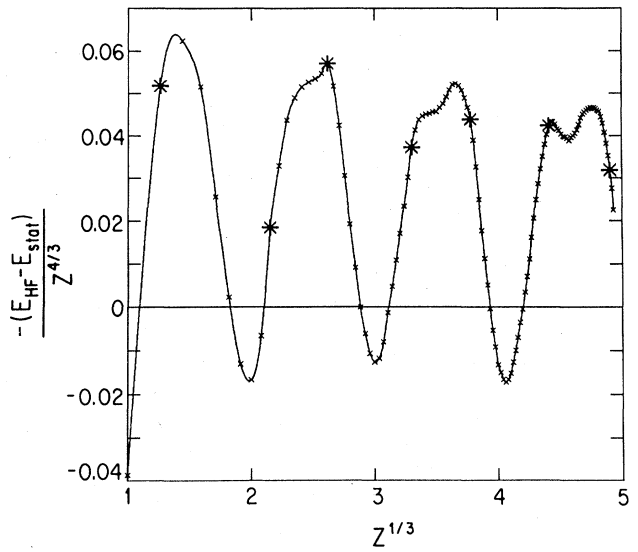

FIG. 2. Absolute deviation between HF binding energies and the statistical formula (1), divided by $Z^{4/3}$, as a function of $Z^{1/3}$. Stars mark closed-shell atoms.

does not explain a single quantitative detail. In fact, as a class, the closed-shell atoms ($Z=2$, 10, 18, 36, 54, 86, and 118) do not reside on prominent sites of the HF curve, as shown in Fig. 2. Strongly pronounced shell effects do exist in Coulombic potentials where all electrons of a Bohr shell have identical binding energies. As Fig. 2 of II shows, in this situation the binding-energy oscillations are of the order $Z^{5/3}$ with sharp minima and broad maxima, and the Z values of closed-shell atoms are given by the location of the maxima. In real atoms the closing of a shell is a less dramatic event because energetic degeneracy does not mean identical but merely approximately equal binding energies. Therefore, the filling of shells in real atoms is a much gentler process. As we see in Fig. 2, this has mainly two consequences: The amplitude of the energy oscillations is of the order $Z^{4/3}$, not $Z^{5/3}$; and, while the closed-shell atoms do show a tendency toward the maxima and away from the minima, their Z values are no longer predictable by looking at the plot of the binding-energy oscillations.

EXPERIMENTAL EVIDENCE

Experimental knowledge of total atomic binding energies stems from spectroscopic data, the analysis of which supplies step-by-step ionization energies.[9] Unfortunately, this has produced binding energies only up to $Z=20$. For more massive atoms, the ionization potentials after the first 20 electrons are rarely known. In short, we can compare $E_{\rm stat}$ of (1) with reality only for the first 20 members of the Periodic Table. This is done in Fig. 3,

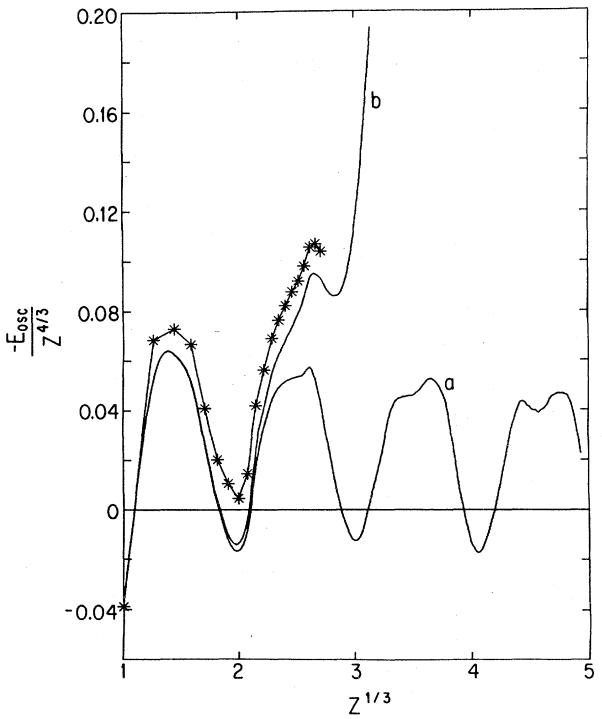

FIG. 3. Binding-energy oscillations. Stars are experimental values for $Z=1,\ldots,20$. Curve *a* shows the nonrelativistic HF oscillation of Fig. 2. Curve *b* connects HF values with relativistic corrections.

where $E_{\rm osc}$ denotes the additive supplement of $E_{\rm stat}$,

$$E=E_{\rm stat}+E_{\rm osc}\ . \tag{2}$$

This figure displays, besides the experimental data, also the nonrelativistic HF oscillations of Fig. 2 and, for $Z\lesssim 31$, the results of HF calculations with relativistic corrections.[4] Please observe two things. First, the experimental values do confirm the existence of binding-energy oscillations. Second, there is, on this scale, a significant discrepancy between experiment and the HF values, even after including relativistic effects. This is a reminder that the HF model is not exact; it is an approximation, just as the TF model is. However, the general trend of the experimental crosses is quite well reproduced by the relativistic HF results, so that we can be sure that the oscillations in question are of nonrelativistic origin. It is therefore appropriate to compare the outcome of our nonrelativistic calculation with the HF oscillations of Fig. 2.

For large values of Z, the relativistic corrections are, evidently, more important than the nonrelativistic oscillations that we are addressing in this paper. There have been attempts to evaluate the relativistic supplement to Eq. (1),[10] none of which has been really satisfactory, so far. We shall return to this subject elsewhere and want to remark now only that the simple estimate[11]

$$\frac{-\Delta E_{\rm rel}}{Z^{4/3}}\cong(4\times10^{-6})Z^{19/6} \tag{3}$$

accounts rather well for the relativistic corrections to the HF values in Fig. 3. Since this figure may create the wrong impression that relativistic effects dominate at large values of Z, we note that even in uranium the relativistic correction amounts to less than 10% of the total binding energy.[4] According to Scott,[11] a rule of thumb says that "the error in the total binding energy resulting from neglecting relativity is roughly $(Z/30)^2\%$."

For small values of Z, the discrepancy between experiment and the HF values cannot be attributed to relativistic corrections. Instead, we see here the limitations of the average potential approach. It does not include electron correlations, which are generally, and quite correctly, made responsible for the difference between $E_{\rm exp}$ and $E_{\rm HF}$ in Fig. 3. On the other hand, the finite mass of the nucleus does not cause any significant correction to the binding energy, except for hydrogen where the effect is relatively largest, about one-twentieth of a percent. For $Z=20$, calcium, its relative size is smaller than that by roughly a factor of 200.[12]

PERTURBATIVE APPROACH

According to I, the nonrelativistic energy of an atom with nuclear charge Z and N electrons is given by

$$E=E_{\rm TF}+E_{\rm qu}\ , \tag{4}$$

where

$$E_{\mathrm{TF}}=\int (d\mathbf{r})\left[-\frac{1}{15\pi^2}\right][-2(V+\zeta)]^{5/2} -\zeta N-\int (d\mathbf{r})\frac{1}{8\pi}\left[\nabla\left[V+\frac{Z}{r}\right]\right]^2 . \tag{5}$$

The quantum correction to the TF energy is, in the Fourier formulation of I,

$$E_{\mathrm{qu}}=4\sum_{k,j=-\infty}^{\infty}{}' (-1)^{k+j} \times\int_0^\infty d\lambda\,\lambda e^{2\pi ik\lambda} \times\int_0^\infty d\nu\, e^{2\pi ij\nu} \times(\varepsilon_{\lambda,\nu}+\zeta)\eta(-\varepsilon_{\lambda,\nu}-\zeta) . \tag{6}$$

Note that the sum over k,j is primed in order to indicate the deletion of the $j=k=0$ term, which is already present in (4) as the first term on the right-hand side.

The energy of Eqs. (4)—(6) does not include exchange effects, which were partly responsible for the last term in Eq. (1). Consequently, neutral atom binding energies derived from this energy functional do not possess the correct $Z^{5/3}$ term. Nevertheless, the leading oscillatory term, the one we are interested in now, will be given correctly, because energy oscillations that grow out of exchange are expected to be smaller by a factor $Z^{2/3}$ $(=Z^{7/3}/Z^{5/3})$ compared to the oscillations produced by direct electrostatic interaction.

For given Z and N, the energy of Eq. (4) is stationary for the correct potential V and the correct value of ζ [cf. Eq. (9) of I]. Also, E_{TF} alone has a stationary property; it is optimized, for neutral atoms ($Z=N$), by the TF potential V_{TF} and $\zeta=0$.[13] Now recall the observation of I that, with this ζ and V, the leading oscillation in E_{qu} is relatively small at sufficiently large Z. All this means that we are justified in evaluating E_{osc} perturbatively by simply inserting $\zeta=0$ and $V=V_{\mathrm{TF}}$ into (6). In other words, we are going to extract E_{osc} out of

$$E_{\mathrm{qu}}=4\sum_{k,j=-\infty}^{\infty}{}' (-1)^{k+j}\int_0^\infty d\lambda\,\lambda e^{2\pi ik\lambda} \times\int_0^\infty d\nu\, e^{2\pi ij\nu} \times\varepsilon_{\lambda,\nu}\eta(-\varepsilon_{\lambda,\nu}) , \tag{7}$$

with $\varepsilon_{\lambda,\nu}$ related to the TF potential via Eq. (24) of I. As in I and II, we shall prefer to first compute

$$N_{\mathrm{qu}}(\varepsilon)=4\sum_{k,j=-\infty}^{\infty}{}' (-1)^{k+j}\int_0^{\lambda_\varepsilon} d\lambda\,\lambda e^{2\pi ik\lambda} \times\frac{e^{2\pi ij\nu_\varepsilon(\lambda)}-1}{2\pi ij} , \tag{8}$$

which then produces E_{qu} through integration,

$$E_{\mathrm{qu}}=-\int_{-\infty}^0 d\varepsilon\, N_{\mathrm{qu}}(\varepsilon) \tag{9}$$

[cf. Eqs. (29) and (32) of I]. In Eq. (8), $\nu_\varepsilon(\lambda)$ denotes the lines of degeneracy belonging to the TF potential, defined in Eq. (58) of I and plotted in Fig. 1 of I.

Here then is an outline of the following sections. First, we study the consequences of the quantization of angular motion only and exhibit its leading contribution to E_{osc}. Whereas this can be achieved without any additional approximation, technical complications force us to introduce a suitable approximate treatment, as soon as radial quantization is included. We supply strong evidence in favor of the chosen approximation by demonstrating that it is good enough to produce both the leading and the next-to-leading contributions to E_{osc} from angular quantization. Then we proceed to apply it to the evaluation of the effects of radial quantization. We find three different types of oscillations, which are then investigated separately. Finally, our semiclassical result is compared to the HF prediction in Fig. 12. The differences are accounted for in the discussion section.

l-QUANTIZED THOMAS-FERMI MODEL

We start our survey of $N_{\mathrm{qu}}(\varepsilon)$ and E_{qu} with a look at the $j=0$ terms in the sums of Eqs. (7) and (8). These terms make no reference to the δ function that initially enforced integral values for $n_r=\nu-\frac{1}{2}$ [see Eq. (25) of I]. Consequently, they give the result of improving the TF model by quantization of angular motion *only*, without having radial motion also quantized. We call this the *l*-quantized Thomas-Fermi (*l*TF) model.[14]

Equation (8) is here reduced to

$$[N_{\mathrm{qu}}(\varepsilon)]_{l\mathrm{TF}}=8\sum_{k=1}^{\infty}(-1)^k\int_0^{\lambda_\varepsilon} d\lambda\,\lambda\nu_\varepsilon(\lambda)\cos(2\pi k\lambda) . \tag{10}$$

After inserting $\nu_\varepsilon(\lambda)$ from Eq. (24) of I, and changing the order of integration,

$$[N_{\mathrm{qu}}(\varepsilon)]_{l\mathrm{TF}}=8\sum_{k=1}^{\infty}(-1)^k\frac{1}{\pi} \times\int_0^\infty dr\frac{1}{r}\int_0^{\lambda_\varepsilon(r)} d\lambda\,\lambda[2r^2(\varepsilon-V) -\lambda^2]^{1/2} \times\cos(2\pi k\lambda) . \tag{11}$$

We note that, for given r, the λ integration covers the range

$$0\le\lambda\le[2r^2(\varepsilon-V)]^{1/2}\equiv\lambda_\varepsilon(r) . \tag{12}$$

Upon substituting

$$\lambda=\lambda_\varepsilon(r)\cos\theta , \tag{13}$$

Eq. (11) turns into

$$[N_{\rm qu}(\varepsilon)]_{l\rm TF}=8\sum_{k=1}^{\infty}(-1)^k\int_0^\infty dr\frac{1}{r}[\lambda_\varepsilon(r)]^3\left[\frac{1}{\pi}\int_0^{\pi/2}d\theta\cos\theta\sin^2\theta\cos[2\pi k\lambda_\varepsilon(r)\cos\theta]\right]. \tag{14}$$

The definition of $\lambda_\varepsilon(r)$ in (12) implies

$$\frac{d}{d\varepsilon}\lambda_\varepsilon(r)=\frac{r^2}{\lambda_\varepsilon(r)}\,, \tag{15}$$

which is used in recognizing the identity

$$[\lambda_\varepsilon(r)]^3\cos\theta\sin^2\theta\cos[2\pi k\lambda_\varepsilon(r)\cos\theta]$$
$$=\frac{d}{d\varepsilon}\left[\frac{1}{3r^2}[\lambda_\varepsilon(r)]^5\cos\theta\sin^4\theta\cos[2\pi k\lambda_\varepsilon(r)\cos\theta]\right]+\tfrac{1}{3}[\lambda_\varepsilon(r)]^3\frac{d}{d\theta}\{\cos^2\theta\sin^3\theta\cos[2\pi k\lambda_\varepsilon(r)\cos\theta]\}\,. \tag{16}$$

Since the last term does not contribute to the θ integration in (14), the ε integration of (9) is now immediate, resulting in[15]

$$(E_{\rm qu})_{l\rm TF}=-\frac{8}{3\pi}\sum_{k=1}^{\infty}(-1)^k\int_0^\infty dr\frac{1}{r^3}[\lambda_0(r)]^5\int_0^{\pi/2}d\theta\cos\theta\sin^4\theta\cos[2\pi k\lambda_0(r)\cos\theta]\,. \tag{17}$$

The outcomes of the θ integrations in (14) and (17) can be expressed in terms of Struve functions[16] (which are close relatives of Bessel functions). For example,

$$\int_0^{\pi/2}d\theta\cos\theta\sin^4\theta\cos[2\pi k\lambda_0(r)\cos\theta]$$
$$=\frac{1}{5}-\frac{3}{8\pi}\left[\frac{1}{k\lambda_0(r)}\right]^2\mathbf{H}_3(2\pi k\lambda_0(r))\,. \tag{18}$$

The detailed information contained in (17) and (18) is of no interest to us here; what we want to know is the leading oscillatory contribution of $(E_{\rm qu})_{l\rm TF}$ for Z sufficiently large that our perturbative evaluation is justified. Recall that the scaling properties of $V_{\rm TF}$ cause λ_0 to be proportional to $Z^{1/3}$ (see paper I). The same holds for $\lambda_0(r)$. We are, therefore, going to use the asymptotic form of $\mathbf{H}_3$,

$$\mathbf{H}_3(z)\sim\sqrt{2/(\pi z)}\sin\left[z+\frac{\pi}{4}\right]+\frac{2}{15\pi}z^2+\frac{1}{\pi}+\cdots\,, \tag{19}$$

in (18), and then (17), in order to establish the large-Z version of Eq. (17):

$$(E_{\rm qu})_{l\rm TF}\cong\frac{1}{\pi^3}\sum_{k=1}^{\infty}\frac{(-1)^k}{k^{5/2}}\int_0^\infty dr\frac{1}{r^3}[\lambda_0(r)]^{5/2}\times\sin\left[2\pi k\lambda_0(r)+\frac{\pi}{4}\right]. \tag{20}$$

The last step in finding the leading lTF oscillation is the stationary phase evaluation of the radial integration. According to Eq. (38) of I, $\lambda_0(r)$ has a maximum at $r=r_0$, around which

$$\lambda_0(r)\cong\lambda_0-\frac{1}{4}\frac{\omega_0^2}{\lambda_0}(r-r_0)^2\,. \tag{21}$$

Consequently, the leading contribution to $E_{\rm osc}$ from $(E_{\rm qu})_{l\rm TF}$ is

$$\frac{1}{\pi^3}\sum_{k=1}^{\infty}\frac{(-1)^k}{k^{5/2}}\frac{\lambda_0^{5/2}}{r_0^3}\times\int dr\sin\left[2\pi k\lambda_0-\tfrac{1}{2}\pi k\frac{\omega_0^2}{\lambda_0}(r-r_0)^2+\frac{\pi}{4}\right]$$
$$=\sqrt{2}\frac{\lambda_0^3}{r_0^3\omega_0}\sum_{k=1}^{\infty}\frac{(-1)^k}{(\pi k)^3}\sin(2\pi k\lambda_0)\,. \tag{22}$$

In anticipation of the sequel we introduce for any ε

$$\nu'_\varepsilon\equiv-\frac{\partial\nu_\varepsilon(\lambda)}{\partial\lambda}\bigg|_{\lambda=\lambda_\varepsilon}=\sqrt{2}\frac{\lambda_\varepsilon}{\omega_\varepsilon r_\varepsilon} \tag{23}$$

[cf. Eq. (42) of I] and, as in II,

$$\dot\lambda_\varepsilon\equiv\frac{d}{d\varepsilon}\lambda_\varepsilon=r_\varepsilon^2/\lambda_\varepsilon \tag{24}$$

[cf. Eq. (37) of I], so that the lTF contribution to $E_{\rm osc}$ is expressed by

$$(-E_{\rm osc})_{l\rm TF}=-\frac{\lambda_0\nu'_0}{\dot\lambda_0}\sum_{k=1}^{\infty}\frac{(-1)^k}{(\pi k)^3}\sin(2\pi k\lambda_0)+\cdots\,; \tag{25}$$

the ellipsis is a reminder of the omitted oscillatory terms, which have amplitudes that are smaller than the displayed leading one, by powers of $Z^{1/3}$.

We recognize the sum over k in (25) to be of the type listed in (29) of II. This, and use of the numbers reported in (61) of I, which we supplement with

$$\dot\lambda_0=\frac{r_0^2}{\lambda_0}=3.739\,20Z^{-3/3}\,, \tag{26}$$

produces finally

$$\left[\frac{-E_{\rm osc}}{Z^{4/3}}\right]_{l\rm TF}=0.320\,594\langle\lambda_0\rangle(\tfrac{1}{4}-\langle\lambda_0\rangle^2)+\cdots\,, \tag{27}$$

where

$$\lambda_0=0.927\,992Z^{1/3}\,. \tag{28}$$

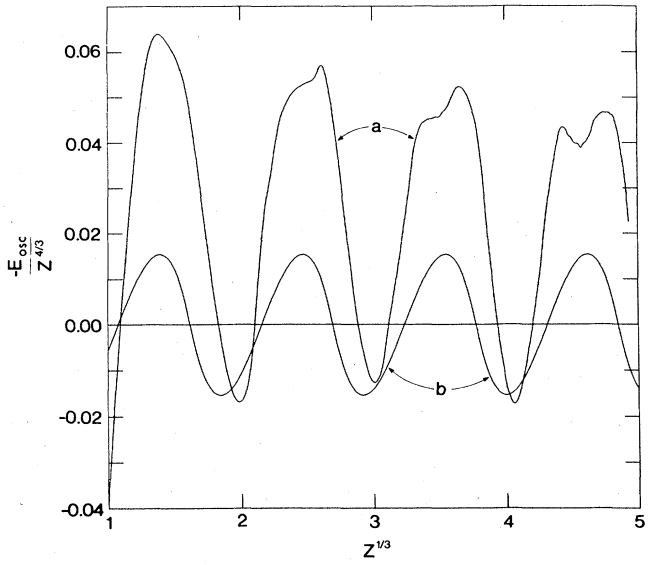

FIG. 4. Comparison of HF oscillations (curve *a*) with leading *l*TF oscillation (curve *b*).

This leading *l*TF energy oscillation, now extrapolated down to small values of $Z^{1/3}$, is plotted in Fig. 4 along with the HF oscillation of Fig. 2. It shows the *l*TF model is responsible for about one-half of the energy oscillation; the other half is expected to be accounted for by radial quantization. Certainly, the phase and the period of the *l*TF oscillation are correct and so is the Z dependence of the amplitude.

Before going on, we state that, as we shall see below, the next-to-leading *l*TF oscillation is small compared to (27), although not negligible over the range of $Z^{1/3}$ in Fig. 4. This is the justification of interpolating (27) to these small values of $Z^{1/3}$.

*l*TF MODEL AGAIN

While this investigation of the *l*TF model was gratifying, it is a rather elaborate way of arriving at the simple answer (27). We shall now reproduce this result, together with the next-to-leading oscillation, by introducing a sensible approximation right from the beginning. This will lay the ground for the evaluation of the $j\neq 0$ terms of (8) and then (7).

The approximation to be used replaces the exact TF lines of degeneracy by quadratic polynomials,

$$\nu_\varepsilon(\lambda)\cong\nu'_\varepsilon(\lambda_\varepsilon-\lambda)-\tfrac{1}{2}\nu''_\varepsilon(\lambda_\varepsilon-\lambda)^2\,, \tag{29}$$

where λ_ε and ν'_ε have the significance assigned to them earlier, whereas the appropriate choice for ν''_ε will become clear later.

With this $\nu_\varepsilon(\lambda)$ the integration over λ in (10) is straightforward; it supplies oscillatory terms from the upper limit. We display the two leading oscillatory terms:

$$[N_{\rm osc}(\varepsilon)]_{l\rm TF}=-2\lambda_\varepsilon\nu'_\varepsilon\sum_{k=1}^{\infty}\frac{(-1)^k}{(\pi k)^2}\cos(2\pi k\lambda_\varepsilon)+(2\nu'_\varepsilon+\lambda_\varepsilon\nu''_\varepsilon)\sum_{k=1}^{\infty}\frac{(-1)^k}{(\pi k)^3}\sin(2\pi k\lambda_\varepsilon)+\cdots\,. \tag{30}$$

We can now perform the ε integration required in (9) analogously to Eq. (77) of I. For example,

$$-\int_{-\infty}^{0}d\varepsilon\,\lambda_\varepsilon\nu'_\varepsilon\cos(2\pi k\lambda_\varepsilon)=\int_{-\infty}^{0}d\varepsilon\frac{d}{d\varepsilon}\left[\lambda_\varepsilon\nu'_\varepsilon\frac{\sin(2\pi k\lambda_\varepsilon)}{2\pi k\dot\lambda_\varepsilon}+\frac{d}{d\varepsilon}\left[\frac{\lambda_\varepsilon\nu'_\varepsilon}{2\pi k\dot\lambda_\varepsilon}\right]\frac{\cos(2\pi k\lambda_\varepsilon)}{2\pi k\dot\lambda_\varepsilon}+\cdots\right]$$
$$=-\frac{1}{2}\frac{\lambda_0\nu'_0}{\dot\lambda_0}\frac{\sin(2\pi k\lambda_0)}{\pi k}-\frac{1}{4}\frac{\lambda_0\nu'_0}{\dot\lambda_0^2}\left[\frac{\dot\lambda_0}{\lambda_0}+\frac{\dot\nu'_0}{\nu'_0}-\frac{\ddot\lambda_0}{\dot\lambda_0}\right]\frac{\cos(2\pi k\lambda_0)}{(\pi k)^2}+\cdots\,. \tag{31}$$

The dots symbolize differentiation with respect to ε, a notation already utilized in (24).

The result for the *l*TF contribution to $E_{\rm osc}$ is then

$$(-E_{\rm osc})_{l\rm TF}=-\frac{\lambda_0\nu'_0}{\dot\lambda_0}\sum_{k=1}^{\infty}\frac{(-1)^k}{(\pi k)^3}\sin(2\pi k\lambda_0)-\frac{1}{2}\frac{\nu'_0}{\dot\lambda_0}\left[3+\frac{\lambda_0\dot\nu'_0}{\dot\lambda_0\nu'_0}-\frac{\lambda_0\ddot\lambda_0}{\dot\lambda_0^2}+\frac{\lambda_0\nu''_0}{\nu'_0}\right]\times\sum_{k=1}^{\infty}\frac{(-1)^k}{(\pi k)^4}\cos(2\pi k\lambda_0)+\cdots\,; \tag{32}$$

again, we report just the two leading terms. And for good reason, because the structure of (32) indicates that the next term would have an amplitude containing also third derivatives—$\dddot\lambda_0$, $\dddot\nu'_0$, $\dddot\nu''_0$, ν'''_0—so that the approximation (29) is bound to fail in detail.

Equation (32) illustrates one of the reasons why we choose a quadratic polynomial for the approximation of $\nu_\varepsilon(\lambda)$; we would not have obtained the next-to-leading oscillation correctly with a linear one. A linear approximation is also prohibited by the observation of II that, when radial quantization is included, linear degeneracy gives rise to a binding-energy oscillation which has an amplitude proportional to $Z^{5/3}$—too large an order for the TF potential, for which the leading oscillation is *known* (see I)

to be of lesser order in $Z^{1/3}$.

When introducing the approximation (29), we were not specific about ν_ε''. Evidently, inasmuch as (29) is the beginning of a power series in $\lambda_\varepsilon-\lambda$, we have

$$\nu_\varepsilon''=-\frac{\partial^2}{\partial\lambda^2}\nu_\varepsilon(\lambda)\bigg|_{\lambda=\lambda_\varepsilon}, \tag{33}$$

which we need for $\varepsilon=0$. This second derivative has been worked out in the Appendix of I, with the result

$$\lambda_0\nu_0''=0.193\,647\ . \tag{34}$$

However, Eq. (29) is *not* a power series in $\lambda_\varepsilon-\lambda$; it stops at the quadratic term. We are therefore well advised to not use ν_ε'' of (33) since it could lead to a poor approximation for λ not close to λ_ε. Two basic properties of $\nu_\varepsilon(\lambda)$ offer themselves for providing a suitable value for ν_0''. One is the TF number count, Eq. (33) of I,

$$Z=N_{\rm TF}(\varepsilon=0)=4\int_0^{\lambda_0}d\lambda\,\lambda\nu_0(\lambda)\ . \tag{35}$$

For $\nu_0(\lambda)$ of (29) this means

$$Z=\tfrac{2}{3}\lambda_0^3\nu_0'-\tfrac{1}{6}\lambda_0^4\nu_0''\ , \tag{36}$$

or

$$\lambda_0\nu_0''=4\nu_0'-6Z/\lambda_0^3=0.242\,810\ . \tag{37}$$

The other one is the initial slope, for which we write

$${}'\nu_\varepsilon\equiv-\frac{\partial}{\partial\lambda}\nu_\varepsilon(\lambda)\bigg|_{\lambda=0}, \tag{38}$$

a notation that is to be contrasted with that of (23). According to Eq. (49) of I, ${}'\nu_\varepsilon$ equals unity for $\varepsilon<0$, while it is $\frac{3}{2}$ for $\varepsilon=0$ for the TF potential. This property of the TF potential, however, can hardly be taken seriously, since it refers to the unrealistically slow decrease of the potential at large distances. Any realistic potential has ${}'\nu_0=1$.

Inserting (29) into (38) produces

$${}'\nu_\varepsilon=\nu_\varepsilon'-\lambda_\varepsilon\nu_\varepsilon''\ , \tag{39}$$

thus

$$\lambda_0\nu_0''=\nu_0'-{}'\nu_0=\begin{cases}0.937\,68 & \text{for } {}'\nu_0=1\ ,\\ 0.437\,68 & \text{for } {}'\nu_0=\frac{3}{2}\ .\end{cases} \tag{40}$$

So we have a choice of three (or even four) values for ν_0''. Which one to use? As far as the lTF model is concerned, one can easily imagine continuing the power series that begins in (29), and certainly the ν_0'' of (34) would then produce the correct amplitude of the next-to-leading lTF oscillation. However, as soon as radial quantization is included, imagination will not do. We have to stick to (29) as it stands in order to be able to handle the calculation technically. This will become clearer in the next section. There we shall also see that an important role is played by the slopes ν_0' and ${}'\nu_0$—we had better have their values right. This chooses ν_0'' of (40) where the physical option is for ${}'\nu_0=1$. Fine, but should not the approximation for $\nu_\varepsilon(\lambda)$ be such that it reproduces the leading TF term of $N(\varepsilon)=N_{\rm TF}(\varepsilon)+N_{\rm qu}(\varepsilon)$ correctly? Yes, in principle, but one adjustable parameter cannot do *all* these things. We have to make a choice, and we opt for the upper value in (40) when including radial quantization in the following sections. Here, for the lTF model only, (34) is the most natural value, but the other choices would not produce significant changes (see below).

For the numerical evaluation of the amplitude of the next-to-leading lTF oscillation in (32) we need $\ddot\lambda_0$ and $\dot\nu_0'$ for the TF potential. Differentiation of Eq. (72) of II, combined with both Eq. (40) of I and Eq. (23), produces immediately

$$\frac{\lambda_\varepsilon\ddot\lambda_\varepsilon}{\dot\lambda_\varepsilon^2}=4(\nu_\varepsilon')^2-1\ , \tag{41}$$

so that, for the TF potential,

$$\frac{\lambda_0\ddot\lambda_0}{\dot\lambda_0^2}=4(\nu_0')^2-1=14.0184\ . \tag{42}$$

Equations (75) and (76) of II can be slightly rewritten in the forms

$$\frac{\lambda_\varepsilon\dot\nu_\varepsilon'}{\dot\lambda_\varepsilon\nu_\varepsilon'}=1-2(\nu_\varepsilon')^2-\tfrac{1}{4}(\nu_\varepsilon')^2\frac{d}{d\varepsilon}\omega_\varepsilon^2 \tag{43}$$

and

$$\frac{1}{4}\frac{d}{d\varepsilon}\omega_\varepsilon^2=2\frac{r_\varepsilon^2}{\omega_\varepsilon^2}\left[3+r_\varepsilon\frac{d}{dr_\varepsilon}\right]\frac{1}{r_\varepsilon}\frac{d^2}{dr_\varepsilon^2}[r_\varepsilon V(r_\varepsilon)]-(\nu_\varepsilon')^2\ . \tag{44}$$

If we now employ the differential equation obeyed by the TF potential,

$$\frac{1}{r}\frac{d^2}{dr^2}(rV)=-\frac{4}{3\pi}(-2V)^{3/2}\ , \tag{45}$$

and utilize the defining equation of r_ε [Eq. (35) of I], then (44) appears as

$$\frac{1}{4}\frac{d}{d\varepsilon}\omega_\varepsilon^2=\frac{16}{\pi}\frac{\varepsilon}{\omega_\varepsilon^2}r_\varepsilon^2[-2V(r_\varepsilon)]^{1/2}-(\nu_\varepsilon')^2\ . \tag{46}$$

Thus for $\varepsilon=0$,[17]

$$\frac{1}{4}\frac{d}{d\varepsilon}\omega_\varepsilon^2\bigg|_{\varepsilon=0}=-(\nu_0')^2\ , \tag{47}$$

which inserted into Eq. (40) produces

$$\frac{\lambda_0\dot\nu_0'}{\dot\lambda_0\nu_0'}=[(\nu_0')^2-1]^2=7.587\,81\ . \tag{48}$$

The last ingredient in writing (32) analogously to (27) is

$$\sum_{k=1}^{\infty}\frac{(-1)^k}{(\pi k)^4}\cos(2\pi k\lambda_0)=\tfrac{1}{90}-\tfrac{1}{3}(\tfrac{1}{4}-\langle\lambda_0\rangle^2)^2\ , \tag{49}$$

which supplements (29) of II. Here, then, are the two leading lTF energy oscillations:

$$\left[\frac{-E_{\rm osc}}{Z^{4/3}}\right]_{l\rm TF}=0.320\,594\langle\lambda_0\rangle(\tfrac{1}{4}-\langle\lambda_0\rangle^2)$$
$$+0.287\,660Z^{-1/3}$$
$$\times[\tfrac{1}{30}-(\tfrac{1}{4}-\langle\lambda_0\rangle^2)^2]+\cdots\ . \qquad (50)$$

The numerical factor of the next-to-leading oscillation here goes with the natural lTF choice for ν_0'', Eq. (34). The other values of ν_0'' in Eqs. (37) and (40) would replace this number by 0.285 469, 0.254 497, or 0.276 783, respectively.

Figure 5 demonstrates that, as anticipated at the end of the preceding section, the next-to-leading lTF oscillation constitutes a small correction to the leading one. The sum of both has the overall characteristics of the leading lTF oscillation [see the paragraph following Eq. (28)], the main difference appearing at $Z^{1/3}\lesssim 2$. It is reassuring that (50) is somewhat better in this range than is (27). (Incidentally, the use of the other values of ν_0'' would not cause a visible change in Fig. 5.)

So much about the lTF model, i.e., the $j=0$ terms in the sums of Eqs. (7) and (8). It is time now to turn to the

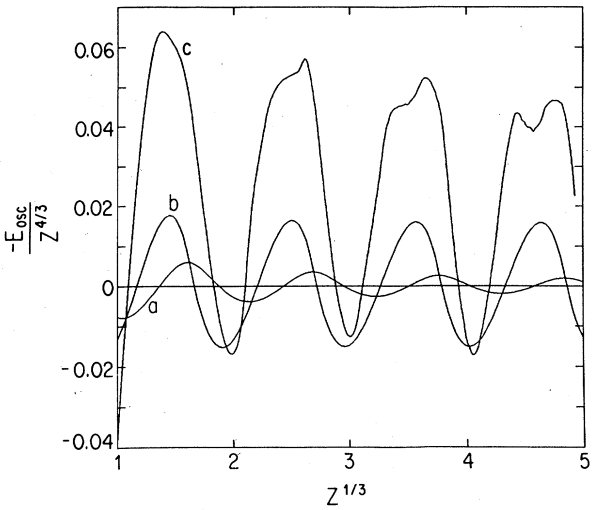

FIG. 5. Next-to-leading lTF oscillation (curve a) and leading plus next-to-leading lTF oscillation (curve b), compared to HF oscillation (curve c).

$j\neq 0$ contributions. For these, the arguments that led to (17) [and then (20), etc.] cannot be repeated. We shall, therefore, right from the start introduce the approximation for $\nu_\varepsilon(\lambda)$ given in Eq. (29).

FRESNEL INTEGRALS

The -1 that comes with $\exp[2\pi ij\nu_\varepsilon(\lambda)]$ in Eq. (8) does not contribute to the $j\neq 0$ sum because what is summed over is odd in j. Consequently, we have

$$[N_{\rm qu}(\varepsilon)]_{j\neq 0}=4\sum_{j(\neq 0)}\sum_{k=-\infty}^{\infty}\frac{(-1)^{k+j}}{2\pi ij}\int_0^{\lambda_\varepsilon}d\lambda\,\lambda\exp\{2\pi i[k\lambda+j\nu_\varepsilon(\lambda)]\}$$
$$=4\,\mathrm{Re}\left[\sum_{j=1}^{\infty}\sum_{k=-\infty}^{\infty}\frac{(-1)^{k+j}}{\pi ij}\int_0^{\lambda_\varepsilon}d\lambda\,\lambda\exp\{2\pi i[k\lambda+j\nu_\varepsilon(\lambda)]\}\right]. \qquad (51)$$

The last form has the advantage that, after inserting $\nu_\varepsilon(\lambda)$ from (29), the term quadratic in λ in the exponent has a definite sign. With this $\nu_\varepsilon(\lambda)$, the combination $k\lambda+j\nu_\varepsilon(\lambda)$ has a maximum at $\lambda=\bar\lambda$ given by

$$\bar\lambda=\lambda_\varepsilon+\frac{1}{j\nu_\varepsilon''}(k-j\nu_\varepsilon')=\frac{1}{j\nu_\varepsilon''}[k-j(\nu_\varepsilon'-\lambda_\varepsilon\nu_\varepsilon'')]\ . \qquad (52)$$

Here and in the sequel we leave the dependence of $\bar\lambda$ on ε, j, and k implicit.

In the last version of (52) we recognize $'\nu_\varepsilon$ of (39), so that $\bar\lambda$ and $\bar\lambda-\lambda_\varepsilon$ are related to $'\nu_\varepsilon$ and ν_ε', respectively, in an identical manner:

$$\bar\lambda=\frac{1}{j\nu_\varepsilon''}(k-j\,'\nu_\varepsilon)\ ,$$
$$\bar\lambda-\lambda_\varepsilon=\frac{1}{j\nu_\varepsilon''}(k-j\nu_\varepsilon')\ . \qquad (53)$$

The significance of these equations consists in their informing us that $\bar\lambda$, the point of stationary phase, lies within the range covered by the λ integration only if

$$j\,'\nu_\varepsilon\leq k\leq j\nu_\varepsilon'\ . \qquad (54)$$

Consequently, for such j and k the value of the λ integral in (51) is expected to be large. Here we see the importance of using an approximation for $\nu_\varepsilon(\lambda)$ which possesses the correct slopes at both ends, as we anticipated in the preceding section when opting for ν_0'' of Eq. (40). As mentioned there, the physically preferable value for $'\nu_0$ is unity, so that, for $\varepsilon=0$,

$$j\leq k\leq 1.937\,68j \qquad (55)$$

is the range of k for which $0\leq\bar\lambda\leq\lambda_0$.

After utilizing $\bar\lambda$ in writing

$$k\lambda+j\nu_\varepsilon(\lambda)=k\bar\lambda+j\nu_\varepsilon(\bar\lambda)-\tfrac{1}{2}j\nu_\varepsilon''(\lambda-\bar\lambda)^2$$
$$=k\lambda_\varepsilon+\tfrac{1}{2}j\nu_\varepsilon''(\lambda_\varepsilon-\bar\lambda)^2-\tfrac{1}{2}j\nu_\varepsilon''(\lambda-\bar\lambda)^2\ , \qquad (56)$$

Eq. (51) becomes

$$[N_{\rm qu}(\varepsilon)]_{j\neq 0}=4\,\mathrm{Re}\left[\sum_{j=1}^{\infty}\sum_{k=-\infty}^{\infty}\frac{(-1)^{k+j}}{\pi ij}\exp\{2\pi i[k\lambda_\varepsilon+\tfrac{1}{2}j\nu_\varepsilon''(\lambda_\varepsilon-\bar\lambda)^2]\}\int_0^{\lambda_\varepsilon}d\lambda\,\lambda\exp[-\pi ij\nu_\varepsilon''(\lambda-\bar\lambda)^2]\right]. \tag{57}$$

The weight factor λ in the integral can be equivalently replaced by

$$\lambda\to\bar\lambda-\frac{1}{2\pi ij\nu_\varepsilon''}\frac{\partial}{\partial\lambda} \tag{58}$$

which allows an immediate partial integration. At this stage we have

$$[N_{\rm qu}(\varepsilon)]_{j\neq 0}=4\,\mathrm{Re}\left[\sum_{j=1}^{\infty}\sum_{k=-\infty}^{\infty}\frac{(-1)^{k+j}}{\pi ij}\left[\frac{\exp[2\pi ij\nu_\varepsilon(0)]-\exp(2\pi ik\lambda_\varepsilon)}{2\pi ij\nu_\varepsilon''}+\bar\lambda\exp\{2\pi i[k\bar\lambda+j\nu_\varepsilon(\bar\lambda)]\}\int_0^{\lambda_\varepsilon}d\lambda\exp[-\pi ij\nu_\varepsilon''(\lambda-\bar\lambda)^2]\right]\right]. \tag{59}$$

The remaining integral is of Fresnel type. Its standard form is[18]

$$\mathrm{E}(z)=\int_0^z dt\exp(-\tfrac{1}{2}\pi it^2)=\mathrm{C}(z)-i\mathrm{S}(z)\,, \tag{60}$$

where the letters E, C, and S refer to the exponential, the cosine, and the sine functions that are integrated. C(z) and S(z) are, of course, real functions. The oscillatory nature of E(z) is made explicit in writing, for $z\geq 0$,

$$\mathrm{E}(z)=\tfrac{1}{2}(1-i)+ih(z)\exp(-\tfrac{1}{2}\pi iz^2)\,, \tag{61}$$

where the slowly varying function $h(z)$ obeys the differential equation

$$h'(z)=\frac{d}{dz}h(z)=\pi izh(z)-i \tag{62}$$

and is subject to

$$h(0)=\tfrac{1}{2}(1+i)\,. \tag{63}$$

In terms of the real and the imaginary parts of $h(z)$ these two equations are expressed by

$$\begin{aligned}&h(z)=f(z)+ig(z)\,,\\ &f'(z)=-\pi zg(z)\,,\quad g'(z)=\pi zf(z)-1\,,\\ &f(0)=g(0)=\tfrac{1}{2}\,.\end{aligned} \tag{64}$$

The asymptotic expansion of $f(z)$ and $g(z)$ can be obtained either by repeated partial integrations in (60) or, equivalently, by iterating (62). The outcome is

$$\begin{aligned}&f(z)\sim\frac{1}{\pi z}-\frac{3}{\pi^3z^5}+\cdots\quad\text{for } z\gg 1\,,\\ &g(z)\sim\frac{1}{\pi^2z^3}-\frac{15}{\pi^4z^7}+\cdots\quad\text{for } z\gg 1\,.\end{aligned} \tag{65}$$

The leading asymptotic terms represent highly accurate approximations already for relatively small z. This is demonstrated both in Table I and in Fig. 6, which also illustrates our statement that $h(z)$ [i.e., $f(z)$ and $g(z)$] is a slowly varying function compared to the exponential in (61).

As defined in (60), E(z) is an odd function of z. Therefore, if we take $h(z)$ to be an odd function,

$$h(z<0)\equiv -h(-z)\,, \tag{66}$$

which is consistent with (62) (for $z\neq 0$), the extension of (61) to include negative values of z then reads

$$\mathrm{E}(z)=\pm\tfrac{1}{2}(1-i)+ih(z)\exp(-\tfrac{1}{2}\pi iz^2)\,, \tag{67}$$

TABLE I. Deviation of leading asymptotic forms from $f(z)$ and $g(z)=-f'(z)/\pi z$.

z	Deviation from $f(z)$ (%)	Deviation from $g(z)$ (%)
1	13.7	64.1
2	1.64	7.82
3	0.36	1.78
4	0.12	0.58
5	0.05	0.24
6	0.02	0.12

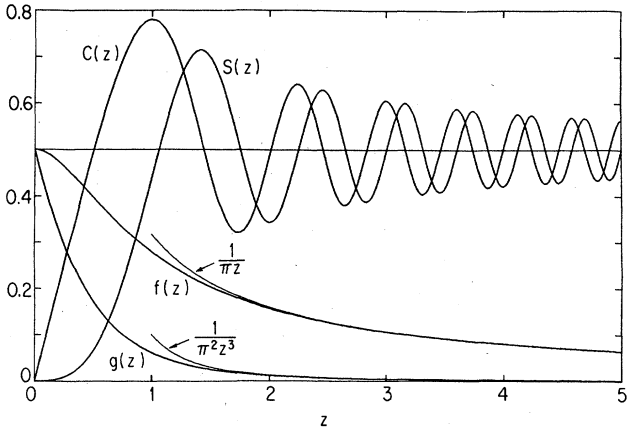

FIG. 6. Fresnel integrals $C(z)$ and $S(z)$; auxiliary functions $f(z)$ and $g(z)$ together with their leading asymptotic forms.

where the lower sign applies for $z<0$. Note that $h(z)$ is discontinuous at $z=0$, where (62) does not apply. Of course, $\mathrm{E}(z)$ itself is perfectly continuous.

For the evaluation of the integral in (59) we introduce $\mathrm{E}(z)$ through the identity

$$\exp[-\pi i j\nu_\varepsilon''(\lambda-\bar{\lambda})^2]=\frac{1}{\sqrt{2j\nu_\varepsilon''}}\frac{d}{d\lambda}\mathrm{E}(\sqrt{2j\nu_\varepsilon''}(\lambda-\bar{\lambda}))\ . \tag{68}$$

This results in

$$[N_{\mathrm{qu}}(\varepsilon)]_{j\neq 0}=4\,\mathrm{Re}\left[\sum_{j=1}^{\infty}\sum_{k=-\infty}^{\infty}\frac{(-1)^{k+j}}{\pi i j}\left[\frac{\exp[2\pi i j\nu_\varepsilon(0)]-\exp(2\pi i k\lambda_\varepsilon)}{2\pi i j\nu_\varepsilon''}+\frac{\bar{\lambda}}{\sqrt{2j\nu_\varepsilon''}}\exp\{2\pi i[k\bar{\lambda}+j\nu_\varepsilon(\bar{\lambda})]\}\right.\right.$$
$$\left.\left.\times[\mathrm{E}(\sqrt{2j\nu_\varepsilon''}(\lambda_\varepsilon-\bar{\lambda}))+\mathrm{E}(\sqrt{2j\nu_\varepsilon''}\bar{\lambda})]\right]\right]\ . \tag{69}$$

The insertion of (67) now shows that $N_{\mathrm{qu}}(\varepsilon)$ consists of three distinct parts which are characterized by their oscillatory behavior, i.e., by the argument of the exponential. *First,* we have from the oscillatory part of the first $\mathrm{E}(\cdots)$

$$\exp\{2\pi i[k\bar{\lambda}+j\nu_\varepsilon(\bar{\lambda})-\tfrac{1}{2}j\nu_\varepsilon''(\lambda_\varepsilon-\bar{\lambda})^2]\}=\exp(2\pi i k\lambda_\varepsilon) \tag{70}$$

[Eq. (56) for $\lambda=\lambda_\varepsilon$]. The periodicity of these terms is given by the maximum value of λ; they lead to λ oscillations. *Second,* analogously the second $\mathrm{E}(\cdots)$ provides terms proportional to

$$\exp\{2\pi i[k\bar{\lambda}+j\nu_\varepsilon(\bar{\lambda})-\tfrac{1}{2}j\nu_\varepsilon''\bar{\lambda}^2]\}=\exp[2\pi i j\nu_\varepsilon(0)] \tag{71}$$

which involve solely the maximum value of ν_ε, therefore supplying ν oscillations. *Third,* there are the constants of (67) in the $\mathrm{E}(\cdots)$'s of (69); because of the two signs in (67) these constants add up to a null result, unless the arguments of the two $\mathrm{E}(\cdots)$'s agree in sign. This is the situation if

$$0\leq\bar{\lambda}\leq\lambda_\varepsilon\ , \tag{72}$$

which is the requirement that $\bar{\lambda}$ lies within the range covered by the λ integration. We have found earlier that, as a consequence of (53), this is equivalent to (54). Accordingly, in this part of $N_{\mathrm{qu}}(\varepsilon)$—referred to as "mixed λ,ν oscillations"—the sum over k is, for each j, limited to a finite range.

The following sections will deal separately with these three different types of oscillations. We shall see that only the λ oscillations are significant for the relatively small values of $Z^{1/3}$ (namely, $1,\ldots,5$) that we are concerned with.

λ OSCILLATIONS

The λ oscillations of $N(\varepsilon)$ are given by

$$[N_{\mathrm{osc}}(\varepsilon)]_\lambda=[N_{\mathrm{osc}}(\varepsilon)]_{l\mathrm{TF}}+2\,\mathrm{Re}\left[\sum_{j=1}^{\infty}\sum_{k(\neq 0)}\frac{(-1)^{k+j}}{(\pi j)^2}\frac{1}{\nu_\varepsilon''}e^{2\pi i k\lambda_\varepsilon}[1+\pi\sqrt{2j\nu_\varepsilon''}\bar{\lambda}h(\sqrt{2j\nu_\varepsilon''}(\lambda_\varepsilon-\bar{\lambda}))]\right]\ , \tag{73}$$

where we have included the lTF oscillation of Eq. (30) and omitted the nonoscillatory $k=0$ terms, such terms being of no interest to us here. As a consequence of the jump of $h(z)$ at $z=0$, $[N_{\mathrm{osc}}(\varepsilon)]_\lambda$ is discontinuous for those values of ε for which λ_ε equals one of the $\bar{\lambda}$. Since the whole $N_{\mathrm{qu}}(\varepsilon)$ is certainly continuous, this discontinuity is not a physical effect, but rather a product of the mathematical separation into the three types of oscillations. In anticipation of the later observation of a compensating discontinuity in the λ,ν oscillations, we shall, for the moment, pretend that all arguments of h (and its derivatives) are nonzero for $\varepsilon\lesssim 0$.

Before exhibiting the real part of (73) explicitly it is advisable to employ the differential equation for h [Eq. (62)] in the form

$$1+\pi\sqrt{2j\nu_\varepsilon''}\bar{\lambda}h(\sqrt{2j\nu_\varepsilon''}(\lambda_\varepsilon-\bar{\lambda}))=ih'(\sqrt{2j\nu_\varepsilon''}(\lambda_\varepsilon-\bar{\lambda}))+\pi\sqrt{2j\nu_\varepsilon''}\lambda_\varepsilon h(\sqrt{2j\nu_\varepsilon''}(\lambda_\varepsilon-\bar{\lambda}))\ . \tag{74}$$

Then we arrive at

$$[N_{\mathrm{osc}}(\varepsilon)]_\lambda=[N_{\mathrm{osc}}(\varepsilon)]_{l\mathrm{TF}}+2\lambda_\varepsilon\sum_{j=1}^{\infty}\sum_{k(\neq 0)}\frac{(-1)^{k+j}}{\pi j}\sqrt{2/(j\nu_\varepsilon'')}f(z_\varepsilon)\cos(2\pi k\lambda_\varepsilon)$$
$$-2\sum_{j=1}^{\infty}\sum_{k(\neq 0)}\frac{(-1)^{k+j}}{\pi j}\bar{\lambda}\sqrt{2/(j\nu_\varepsilon'')}g(z_\varepsilon)\sin(2\pi k\lambda_\varepsilon)-\frac{2}{\nu_\varepsilon''}\sum_{j=1}^{\infty}\sum_{k(\neq 0)}\frac{(-1)^{k+j}}{(\pi j)^2}g'(z_\varepsilon)\cos(2\pi k\lambda_\varepsilon)\ , \tag{75}$$

where z_ε has the significance

$$z_\varepsilon \equiv \sqrt{2j\nu_\varepsilon''}(\lambda_\varepsilon-\bar{\lambda})=\sqrt{2/(j\nu_\varepsilon'')}(j\nu_\varepsilon'-k)\ ; \tag{76}$$

the last equality uses (53).

The three double sums of (75) have differing large-Z behavior. The asymptotic forms of f and g, given in (65), combined with the Z dependences λ_ε, $\bar{\lambda}\sim Z^{1/3}$, $\nu_\varepsilon''\sim Z^{-1/3}$, and $z_\varepsilon\sim Z^{1/6}$, imply that these three terms describe λ oscillations with amplitudes proportional to $Z^{1/3}$, Z^0, and $Z^{-1/3}$, respectively. However, these simple Z dependences of the amplitudes hold only for very large Z; more precisely, they hold when the asymptotic forms of f and g can be used for all j and k to be summed over. For the rather small values of $Z^{1/3}$ we are interested in, there are j,k pairs (mainly the ones with $k=2j$) for which z_ε is not in the asymptotic domain. In other words, while the asymptotics of f and g identify the double sums of (75) to belong to the leading λ oscillation, the next-to-leading one, etc., the extrapolation to the small-$Z^{1/3}$ range is not done correctly if one sticks to these asymptotic forms. Instead, this extrapolation is supplied by use of the full $f(z_\varepsilon)$ and $g(z_\varepsilon)$. Note that the important step in arriving here was the decomposition of the Fresnel integrals into the rapidly oscillating exponential and the slowly varying $h(z)$.

The lTF (or $j=0$) part of (75) is united with the $j\neq 0$ contribution after splitting f and g into their asymptotic forms and the small z correction by writing

$$\begin{aligned} f(z)&=\frac{1}{\pi z}+\tilde{f}(z)\ ,\\ g(z)&=\frac{1}{\pi^2 z^3}+\tilde{g}(z)\ . \end{aligned} \tag{77}$$

We illustrate this unification for the leading λ oscillation. It is given by [Eqs. (30) and (77) in (75)]

$$[N_{\rm osc}(\varepsilon)]_\lambda=-2\lambda_\varepsilon\nu_\varepsilon'\sum_{k=1}^{\infty}\frac{(-1)^k}{(\pi k)^2}\cos(2\pi k\lambda_\varepsilon)+2\lambda_\varepsilon\sum_{j=1}^{\infty}\sum_{k(\neq 0)}\frac{(-1)^{k+j}}{\pi j}\frac{1}{\pi j\nu_\varepsilon'-\pi k}\cos(2\pi k\lambda_\varepsilon)$$
$$+2\lambda_\varepsilon\sum_{j=1}^{\infty}\sum_{k(\neq 0)}\frac{(-1)^{k+j}}{\pi j}\sqrt{2/(j\nu_\varepsilon'')}\tilde{f}(z_\varepsilon)\cos(2\pi k\lambda_\varepsilon)+\cdots\ , \tag{78}$$

where the ellipsis represents the nonleading λ oscillations. The second term in (78) can be rewritten with the aid of the first equation of (24) of II,

$$2\lambda_\varepsilon\sum_{j=1}^{\infty}\sum_{k(\neq 0)}\frac{(-1)^{k+j}}{\pi j}\frac{1}{\pi j\nu_\varepsilon'-\pi k}\cos(2\pi k\lambda_\varepsilon)=\lambda_\varepsilon\sum_{k(\neq 0)}\frac{(-1)^k}{\pi k}\cos(2\pi k\lambda_\varepsilon)\sum_{j(\neq 0)}(-1)^j\left[\frac{1}{-\pi j}-\frac{1}{\pi k/\nu_\varepsilon'-\pi j}\right]$$
$$=2\lambda_\varepsilon\nu_\varepsilon'\sum_{k=1}^{\infty}\frac{(-1)^k}{(\pi k)^2}\cos(2\pi k\lambda_\varepsilon)-2\lambda_\varepsilon\sum_{k=1}^{\infty}\frac{(-1)^k}{\pi k}\frac{\cos(2\pi k\lambda_\varepsilon)}{\sin(\pi k/\nu_\varepsilon')}\ ; \tag{79}$$

the first sum over k exactly cancels the lTF term of (78). At this stage we have

$$[N_{\rm osc}(\varepsilon)]_\lambda=-2\lambda_\varepsilon\sum_{k=1}^{\infty}\frac{(-1)^k}{\pi k}\frac{\cos(2\pi k\lambda_\varepsilon)}{\sin(\pi k/\nu_\varepsilon')}+2\lambda_\varepsilon\sum_{k(\neq 0)}\sum_{j=1}^{\infty}\frac{(-1)^{k+j}}{\pi k}\sqrt{2/(j\nu_\varepsilon'')}\tilde{f}(z_\varepsilon)\cos(2\pi k\lambda_\varepsilon)+\cdots\ . \tag{80}$$

The observation that the first term here is the leading λ oscillation in the situation of linear degeneracy [see Eq. (25) of II] identifies the second one as its correction due to the quadratic nature of (29). Indeed, for $\nu_\varepsilon''\to 0$ [$z_\varepsilon\to\infty$, $\tilde{f}(z_\varepsilon)\sim -z_\varepsilon^{-3}$], only the first term of (80) survives.

The steps that led to Eq. (80) can be repeated for the next-to-leading λ oscillation. The result is

$$[N_{\rm osc}(\varepsilon)]_\lambda=[\text{Eq.}(80)]+\sum_{k=1}^{\infty}\frac{(-1)^k}{(\pi k)^2}\frac{\sin(2\pi k\lambda_\varepsilon)}{\sin(\pi k/\nu_\varepsilon')}+\frac{1}{\nu_\varepsilon'}\sum_{k=1}^{\infty}\frac{(-1)^k}{\pi k}\sin(2\pi k\lambda_\varepsilon)\frac{\cos(\pi k/\nu_\varepsilon')}{\sin^2(\pi k/\nu_\varepsilon')}$$
$$+\frac{\lambda_\varepsilon\nu_\varepsilon''}{(\nu_\varepsilon')^3}\sum_{k=1}^{\infty}(-1)^k\sin(2\pi k\lambda_\varepsilon)\frac{\cos^2(\pi k/\nu_\varepsilon')+\frac{1}{2}\sin^2(\pi k/\nu_\varepsilon')}{\sin^3(\pi k/\nu_\varepsilon')}$$
$$-2\sum_{k(\neq 0)}\sum_{j=1}^{\infty}\frac{(-1)^{k+j}}{\pi j}\bar{\lambda}\sqrt{2/(j\nu_\varepsilon'')}\tilde{g}(z_\varepsilon)\sin(2\pi k\lambda_\varepsilon)+\cdots\ ; \tag{81}$$

again, for $\nu_\varepsilon''\to 0$, it reproduces the respective two terms of the linear degeneracy result, Eq. (25) of II.

From these λ oscillations of $N(\varepsilon)$, the λ oscillations of the energy are obtained by integration, as described by Eq. (9). We calculate the two leading terms by partial integration, in the spirit of Eq. (31). This produces

$$\left[\frac{-E_{\rm osc}}{Z^{4/3}}\right]_\lambda=\sum_{k(\neq 0)}s_k\sin(2\pi k\lambda_0)+\frac{1}{Z^{1/3}}\sum_{k\neq 0}c_k\cos(2\pi k\lambda_0)+\cdots\ , \tag{82}$$

where the Z-dependent coefficients s_k and c_k are given by

$$Z^{4/3}s_k=-\frac{1}{2}\frac{\lambda_0}{\dot\lambda_0}\frac{(-1)^k}{(\pi k)^2}\frac{1}{\sin(\pi k/\nu_0')}+\frac{\lambda_0}{\dot\lambda_0}\frac{(-1)^k}{\pi k}\sum_{j=1}^{\infty}\frac{(-1)^j}{\pi j}\sqrt{2/(j\nu_0'')}\,\tilde f(z_0) \tag{83}$$

[Eq. (76): $z_0=\sqrt{2/(j\nu_0'')}(j\nu_0'-k)$], and

$$\begin{aligned}Z^{3/3}c_k=&\frac{1}{4\dot\lambda_0}\left[\frac{\lambda_0\ddot\lambda_0}{\dot\lambda_0^2}-2\right]\frac{(-1)^k}{(\pi k)^3}\frac{1}{\sin(\pi k/\nu_0')}\\&-\frac{1}{4\dot\lambda_0\nu_0'}\left[\frac{\lambda_0\dot\nu_0'}{\dot\lambda_0\nu_0'}+1\right]\frac{(-1)^k}{(\pi k)^2}\frac{\cos(\pi k/\nu_0')}{\sin^2(\pi k/\nu_0')}-\frac{\lambda_0\nu_0''}{4\dot\lambda_0(\nu_0')^3}\frac{(-1)^k}{\pi k}\frac{\cos^2(\pi k/\nu_0')+\frac{1}{2}\sin^2(\pi k/\nu_0')}{\sin^3(\pi k/\nu_0')}\\&-\frac{1}{\dot\lambda_0}\frac{(-1)^k}{\pi k}\sum_{j=1}^{\infty}\frac{(-1)^j}{\pi j}\left[\left[\frac{\lambda_0\ddot\lambda_0}{\dot\lambda^2}-1\right]\frac{1}{\pi k}\frac{\tilde f(z_0)}{\sqrt{2j\nu_0''}}-\lambda_0\sqrt{2/(j\nu_0'')}\,\tilde g(z_0)-\left[\frac{\lambda_0\dot\nu_0'/\dot\lambda_0}{\pi k}+\frac{1}{\pi j}\right]\frac{\tilde f'(z_0)}{\nu_0''}\right].\end{aligned} \tag{84}$$

Please note that, because $\nu_0'=1.93\ldots$, very large values of j and k are required to obtain $z_0=0$. These terms do not contribute significantly to the Fourier sum of Eq. (82). Therefore, our disregarding of the consequences of the discontinuity of $h(z)$ at $z=0$ is, for all practical purposes, harmless (not to mention the possibility that ν_0' is irrational).

Of course, it is not the individual s_k and c_k that are significant, but the combinations s_k-s_{-k} and c_k+c_{-k}. Before we comment on these, let us first answer this question: What has happened to the term proportional to $\dot\nu_0''$ which is produced by the second partial integration on the leading λ oscillation of Eq. (80)? The answer is that it has been discarded after being recognized as belonging to a smaller order in $Z^{1/3}$. Here is how it goes. The contribution to $-E_{\rm osc}$ in question is

$$-E_{\rm osc}=\cdots-\frac{1}{4}\frac{\lambda_0\dot\nu_0''}{\dot\lambda_0^2\nu_0''}\sum_{k(\neq 0)}\frac{(-1)^k}{(\pi k)^2}\cos(2\pi k\lambda_0)\sum_{j=1}^{\infty}\frac{(-1)^j}{\pi j}\sqrt{2/(j\nu_0'')}[\tilde f(z_0)+z_0\tilde f'(z_0)]+\cdots\,. \tag{85}$$

The observation that, for $z_0\neq 0$,

$$\tilde f(z_0)+z_0\tilde f'(z_0)=f(z_0)+z_0f'(z_0)=\frac{1}{\pi}g''(z_0) \tag{86}$$

shows that (85) is not the small-$Z^{1/3}$ correction to an asymptotic term [note that it is g, not $\tilde g$, in (86)], so that the use of $g''(z)\sim 1/z^5$ identifies (85) to be of order $Z^{1/3}$—two factors of $Z^{1/3}$ smaller than the oscillations considered in (82). This fits together with the remark made above [after Eq. (32)] that knowledge of $\dot\nu_0''$ is not needed as long as we are concerned only with the two leading energy oscillations.

According to Fig. 6 and Table I, $\tilde f(z_0)$ and $\tilde g(z_0)$, the differences between f and g and their asymptotic forms, are large only for small values of their arguments. In fact, they are very large for $z_0\cong 0$, i.e., for $j\cong k/\nu_0'$. In Fig. 7 this is a lattice point close to the $z_0=0$ line. Consequently, the s_k and c_k with positive even k are the ones which will differ most from their asymptotic values for the small $Z^{1/3}$ of interest. We use this insight for an approximate evaluation of s_k by discarding the sum over j in Eq. (83), unless k is even and positive, in which event we keep the $j=k/2$ term. Further, since the z_0 of this term is small and negative and since

$$f(z_0\lesssim 0)=-\tfrac{1}{2}+O(z_0^2)\,, \tag{87}$$

we evaluate this $j=k/2$ term by using

$$\tilde f(z_0)=f(z_0)-\frac{1}{\pi z_0}\cong-\frac{1}{2}+\frac{1}{\pi}\left[\frac{\nu_0''}{k}\right]^{1/2}\frac{1}{(2-\nu_0')}\,. \tag{88}$$

This results in

$$Z^{4/3}(s_k-s_{-k})\cong\begin{cases}\dfrac{\lambda_0}{\dot\lambda_0}\dfrac{1}{(\pi k)^2}\dfrac{1}{\sin(\pi k/\nu_0')} & \text{for } k \text{ odd}\,,\\[2ex] -\dfrac{\lambda_0}{\dot\lambda_0}\dfrac{1}{(\pi k)^2}\left[\dfrac{1}{\sin(\pi k/\nu_0')}-\dfrac{(-1)^{k/2}}{\pi k}\dfrac{4}{(2-\nu_0')}+(-1)^{k/2}\dfrac{2}{\sqrt{k\nu_0''}}\right] & \text{for } k \text{ even}\,.\end{cases} \tag{89}$$

The numerical version of this is (recall that $\nu_0'=1.937\,68$)

$$s_k - s_{-k} \cong \begin{cases} \dfrac{0.025\,15}{k^2 \sin(1.621k)} & \text{for } k \text{ odd}, \\ -\dfrac{0.025\,15}{k^2}\left[\dfrac{1}{\sin(1.621k)}(-1)^{k/2}\dfrac{20.43}{k} + (-)^{k/2}\dfrac{1.990Z^{1/6}}{\sqrt{k}}\right] & \text{for } k \text{ even}. \end{cases} \tag{90}$$

In the latter situation the first two terms in the large parentheses are big, but with opposite signs, and tend to cancel, reflecting the circumstances that (89) is finite for $\nu_0' \to 2$. A handier approximation is obtained by making explicit the small difference between 2 and ν_0', as illustrated by

$$\frac{1}{\sin(\pi k/\nu_0')} \cong (-1)^{k/2}\left[\frac{1}{\pi k}\frac{2\nu_0'}{2-\nu_0'} + \frac{1}{6}\pi k \frac{2-\nu_0'}{2\nu_0'}\right]. \tag{91}$$

With this, Eq. (89) yields

$$s_k - s_{-k} \cong \begin{cases} (-1)^{(k-1)/2}\dfrac{0.025\,15}{k^2} & \text{for } k \text{ odd}, \\ (-1)^{k/2}\left[\dfrac{0.016\,01}{k^3} - \dfrac{0.050\,03}{k^{5/2}}Z^{1/6} - \dfrac{0.000\,427}{k}\right] & \text{for } k \text{ even}. \end{cases} \tag{92}$$

A similar evaluation, proceeding from Eq. (84), gives

$$c_k + c_{-k} \cong \begin{cases} (-1)^{(k+1)/2}\left[\dfrac{0.051\,83}{k^3} + \dfrac{0.000\,29}{k}\right] & \text{for } k \text{ odd}, \\ (-1)^{k/2}\left[-\dfrac{0.033\,00}{k^4} + \dfrac{0.011\,17}{k^{7/2}}Z^{1/6} - \dfrac{0.077\,80}{k^{5/2}}Z^{1/2} + \dfrac{0.010\,01}{k^2} - 0.000\,02\right] & \text{for } k \text{ even}. \end{cases} \tag{93}$$

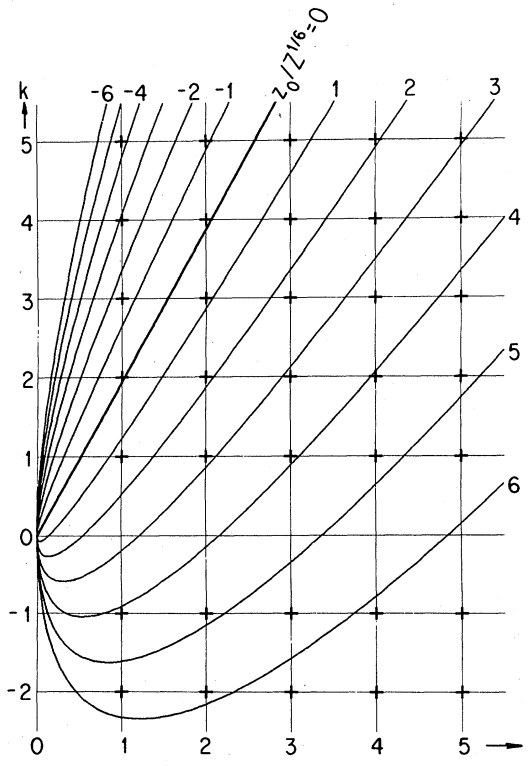

FIG. 7. Curves of constant $z_0/Z^{1/6}$ on the j,k lattice. Crosses mark the lattice points that enter in Eqs. (83) and (84).

Evidently, the approximations employed in arriving at (92) and (93) are such that these expressions are reliable only if neither k nor $Z^{1/6}$ is large. [The failure for large Z is also demonstrated by the fact that the exact s_k and c_k become Z independent for $Z \to \infty$, whereas the even-k ones do not in (92) and (93).] However, this does not seriously limit the applicability of these formulas; the Z values of interest are not large ($Z^{1/6}$: $1 \to 2.2$), and the sums over k in (82) converge rapidly, so that s_k and c_k are needed only for the few first k's. Both these points are illustrated in Figs. 8 and 9 for the s_k and in Figs. 10 and 11 for the c_k. In addition to the fast convergence of the Fourier series (82) and the high quality of (92) and (93), please observe also that in this range of Z the next-to-leading λ oscillation is not dominated by the leading one. They are both of comparable size. Another interesting feature is the growing importance of the even-k terms for increasing Z. This is a consequence of $\nu_0' \cong 2$. For example, when Z becomes very large, the ratio $(s_2 - s_{-2})/(s_1 - s_{-1})$ is 2.48, so that then the dominant period of the oscillations is halved. This effect is even more pronounced for the next-to-leading λ oscillation, as is visible in Fig. 10 and is numerically expressed by $(c_2 + c_{-2})/(c_1 + c_{-1}) = -77.9$ for $Z \to \infty$. However, being suppressed by a factor of $Z^{1/3}$, it is nevertheless small compared to the leading λ oscillation for such enormous values of Z.

ν OSCILLATIONS

The ν oscillations of $N(\varepsilon)$, as obtained from (69), are given by

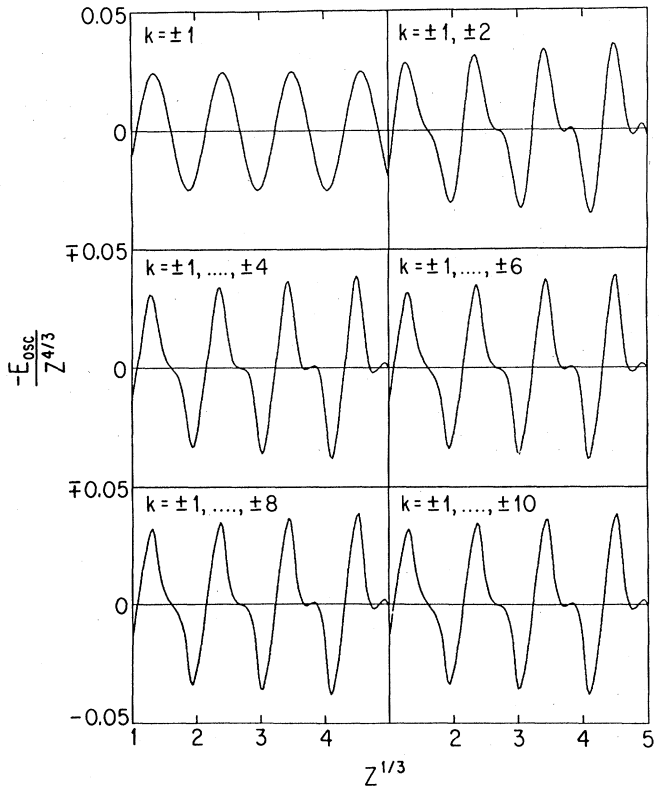

FIG. 8. Partial sums of the leading λ oscillation [first sum in (82)] with s_k from Eq. (83).

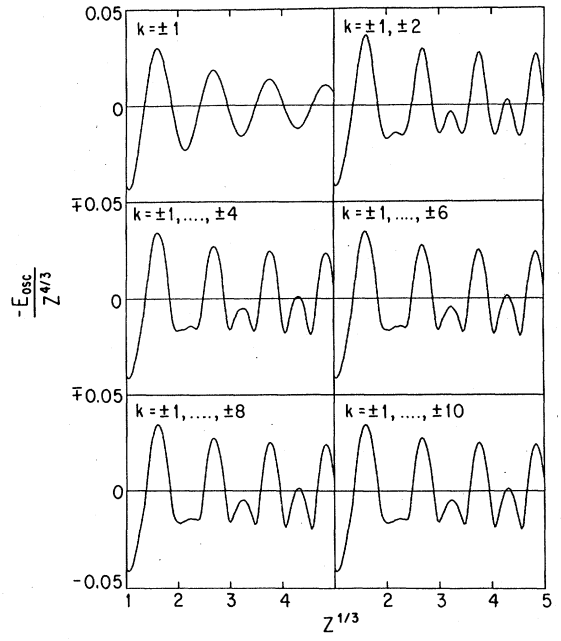

FIG. 10. Partial sums of the next-to-leading λ oscillation [second sum in (82)] with c_k from Eq. (84).

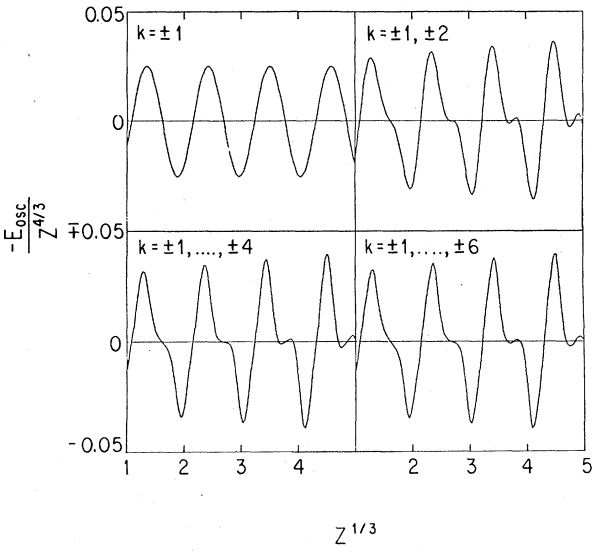

FIG. 9. Like Fig. 8, but using the approximate s_k of (92).

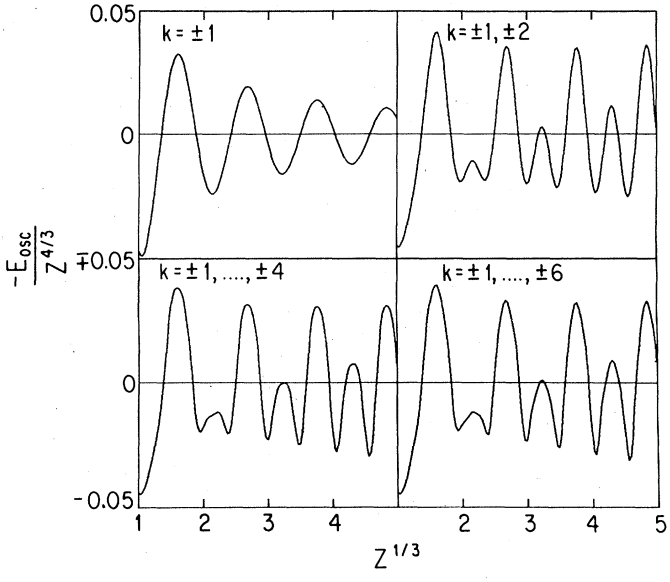

FIG. 11. Like Fig. 10, but using the approximate c_k of (93).

$$[N_{\rm osc}(\varepsilon)]_\nu = 4\,{\rm Re}\left[\sum_{j=1}^{\infty}\sum_{k=-\infty}^{\infty}\frac{(-1)^{k+j}}{\pi ij}\left[\frac{1}{2\pi ij\nu_\varepsilon''}+\frac{\bar\lambda}{\sqrt{2j\nu_\varepsilon''}}ih(\sqrt{2j\nu_\varepsilon''}\,\bar\lambda)\right]e^{2\pi ij\nu_\varepsilon(0)}\right]. \tag{94}$$

Here the discontinuity of $h(z)$ at $z=0$ does not matter, since we encounter the combination $zh(z)$. In view of $\bar\lambda=(k-j)/(j\nu_\varepsilon'')$ [Eq. (53) with $'\nu_\varepsilon\equiv 1$], the $\bar\lambda=0$ terms are given by $k=j$. The $k\neq j$ terms can be rearranged by utilizing the differential equation (62) that is obeyed by $h(z)$ for $z\neq 0$. At this stage, we have

$$[N_{\rm osc}(\varepsilon)]_\nu = \frac{2}{\nu_\varepsilon''}\,{\rm Re}\left[\sum_{j=1}^{\infty}\frac{(-1)^j}{(\pi j)^2}e^{2\pi ij\nu_\varepsilon(0)}\left[-(-1)^j+\sum_{k(\neq j)}(-1)^k\frac{1}{i}h'(\sqrt{2/(j\nu_\varepsilon'')}(k-j))\right]\right]. \tag{95}$$

Now, by setting $m\equiv k-j$ and using $h'(-z)=h'(z)$, this is turned into

$$[N_{\rm osc}(\varepsilon)]_\nu = -\frac{2}{\nu_\varepsilon''}\sum_{j=1}^{\infty}\frac{\cos[2\pi j\nu_\varepsilon(0)]}{(\pi j)^2}+\frac{4}{\nu_\varepsilon''}\,{\rm Re}\left[\sum_{j=1}^{\infty}\frac{e^{2\pi ij\nu_\varepsilon(0)}}{(\pi j)^2}\sum_{m=1}^{\infty}(-1)^m\frac{1}{i}h'(\sqrt{2/(j\nu_\varepsilon'')}m)\right]. \tag{96}$$

In this form the first sum over j is immediately identified as the leading oscillation. Its similarity to the leading lTF oscillation of Eq. (30) is used in writing down the leading ν oscillation of the binding energy:

$$(-E_{\rm osc})_\nu = -\frac{1}{\nu_0''\dot\nu_0(0)}\sum_{j=1}^{\infty}\frac{\sin[2\pi j\nu_0(0)]}{(\pi j)^3}+\cdots. \tag{97}$$

This is of the shape of the leading lTF oscillation [Eq. (25) and Fig. 4] with the period shortened by the fraction (recall that $'\nu_\varepsilon\equiv 1$)

$$\frac{\lambda_0}{\nu_0(0)}=\frac{\lambda_0}{\lambda_0\nu_0'-\frac{1}{2}\lambda_0^2\nu_0''}=\frac{1}{\frac{1}{2}(\nu_0'+{}'\nu_0)}=\frac{1}{1.468\,84} \tag{98}$$

and the amplitude reduced by the factor

$$\frac{1}{\nu_0''\dot\nu_0(0)}\frac{\dot\lambda_0}{\lambda_0\nu_0'}=\frac{2}{\nu_0'[(\nu_0')^2-1][(\nu_0')^4-(\nu_0')^3-(\nu_0')^2+\nu_0'+1]}=\frac{1}{16.0256}. \tag{99}$$

In Eq. (99) we made use of $\lambda_0\nu_0''=\nu_0'-{}'\nu_0=\nu_0'-1$ and

$$\dot\nu_0(0)=\frac{d}{d\varepsilon}[\tfrac{1}{2}\lambda_\varepsilon(\nu_\varepsilon'+{}'\nu_\varepsilon)]\Big|_{\varepsilon=0}=\tfrac{1}{2}[\dot\nu_0'\lambda_0+(\nu_0'+1)\dot\lambda_0]=\tfrac{1}{2}\dot\lambda_0(\nu_0'+1)[(\nu_0')^4-(\nu_0')^3-(\nu_0')^2+\nu_0'+1], \tag{100}$$

where the last step employs (48).

Since, according to Fig. 4, the leading lTF energy oscillation has an amplitude of about $0.015Z^{4/3}$, Eq. (99) implies that the size of the leading ν oscillation of (97) is about $0.001Z^{4/3}$. This is so small compared to the λ oscillations of the preceding section that we shall neglect it entirely. Inasmuch as the discarded subsequent λ oscillations are expected to be larger than the leading ν oscillation (in the small-Z range of interest), this procedure is thoroughly justified.

MIXED λ,ν OSCILLATIONS

Finally, the mixed λ,ν oscillations of $N(\varepsilon)$ [Eq. (69)] are

$$\begin{aligned}[N_{\rm osc}(\varepsilon)]_{\lambda,\nu} &= 4\,{\rm Re}\left[\sum_{j=1}^{\infty}\sum_{k}\frac{(-1)^{k+j}}{\pi ij}\frac{\bar\lambda}{\sqrt{2j\nu_\varepsilon''}}e^{2\pi i[k\bar\lambda+j\nu_\varepsilon(\bar\lambda)]}(1-i)\right]\\ &= -4\sum_{j=1}^{\infty}\sum_{k}\frac{(-1)^{k+j}}{\pi j}\frac{\bar\lambda}{\sqrt{j\nu_\varepsilon''}}\cos\{2\pi[k\bar\lambda+j\nu_\varepsilon(\bar\lambda)]+\tfrac{1}{4}\pi\},\end{aligned} \tag{101}$$

where the summation over k covers the range

$$j={}'j\nu_\varepsilon\le k\le j\nu_\varepsilon'. \tag{102}$$

The lower limit for k does not depend on ε, because $'\nu_\varepsilon\equiv 1$, whereas the upper one does. In particular, when $j\nu_\varepsilon'$ crosses an integer value, the range of the k summation gains one value. In this situation, $\bar\lambda$ equals λ_ε and the discontinuity of $[N_{\rm osc}(\varepsilon)]_{\lambda,\nu}$ is given by

$$\Delta[N_{\rm osc}(\varepsilon)]_{\lambda,\nu} = -4\sum_{j}\frac{(-1)^{j(\nu_\varepsilon'+1)}}{\pi j}\frac{\lambda_\varepsilon}{\sqrt{j\nu_\varepsilon''}}\left[2\pi j\nu_\varepsilon'\lambda_\varepsilon+\frac{\pi}{4}\right], \tag{103}$$

where the summation over j includes all values for which $j\nu_\varepsilon'$ is an integer. (For example, when $\nu_\varepsilon'=\frac{3}{2}$ these are all even j's.) If we now look back at Eq. (73), we see that the

corresponding discontinuity of $[N_{\rm osc}(\varepsilon)]_\lambda$ is

$$\Delta[N_{\rm osc}(\varepsilon)]_\lambda = 2\,{\rm Re}\sum_j \frac{(-1)^{j(\nu'_\varepsilon+1)}}{(\pi j)^2}\frac{1}{\nu''_\varepsilon} \times e^{2\pi i j \nu'_\varepsilon \bar\lambda_\varepsilon}\pi\sqrt{2j\nu''_\varepsilon}(1+i) = -\Delta[N_{\rm osc}(\varepsilon)]_{\lambda,\nu}\,. \tag{104}$$

As anticipated above [see after Eq. (73)], the discontinuities of the λ,ν oscillations exactly compensate for the ones of the λ oscillations, so that we are indeed justified in disregarding them. One could, of course, avoid all these discontinuities by not dealing with the λ and the λ,ν oscillations separately. Recall, however, the remark made after Eq. (84) that, for $\varepsilon=0$, one must go to very large values of j to find an integer value for $j\nu'_0$. Thus, for all practical purposes, these discontinuities are unimportant anyway.

Since $k = j'\nu_\varepsilon$ $(=j)$ implies $\bar\lambda=0$, there is no contribution in (101) for this value of k. On the other hand, ν'_ε does not exceed $\nu'_0=1.93\ldots$. Consequently, there are no $j=1$ terms in (101). For $j=2$ and $\varepsilon\lesssim 0$, the only contribution comes from $k=3$; likewise, for $j=3$, we have nonvanishing terms for $k=4,5$; etc.

The identities

$$\bar\lambda = \frac{1}{j\nu''_\varepsilon}(k - j'\nu_\varepsilon)\,, \qquad k\bar\lambda + j\nu_\varepsilon(\bar\lambda) = \frac{1}{2j\nu''_\varepsilon}\{j^2[(\nu'_\varepsilon)^2-('\nu_\varepsilon)^2]+(k-j'\nu_\varepsilon)^2\} \tag{105}$$

[cf. Eqs. (53) and (56)], combined with $'\nu_\varepsilon\equiv 1$, invite the introduction of a new summation index $m\equiv k-j$, which for each j runs from $m=1$ to $m=M_\varepsilon(j)$, with

$$M_\varepsilon(j)\equiv[j(\nu'_\varepsilon-1)]<j\,. \tag{106}$$

Then the leading λ,ν binding-energy oscillation is

$$(-E_{\rm osc})_{\nu,\lambda} = -\frac{4}{\pi^2}\frac{\sqrt{\nu''_0}}{\dot\nu''_0}\sum_{j=2}^{\infty}\sum_{m=1}^{M_0(j)}\frac{(-1)^m}{j^{3/2}}\left[\left[2\frac{\nu'_0\dot\nu'_0\nu''_0}{\dot\nu''_0}-(\nu'_0)^2+1\right]j^2-m^2\right]^{-1} \times \sin\left[\frac{\pi}{j\nu''_0}\{j^2[(\nu'_0)^2-1]+m^2\}+\frac{\pi}{4}\right]+\cdots\,. \tag{107}$$

Since $\nu''_0\sim 1/Z^{1/3}$ and $\dot\nu''_0\sim 1/Z^{5/3}$, the amplitude of this oscillation is proportional to $Z^{3/2}$. It is therefore *the* leading oscillation. However, we encounter here the situation already mentioned in II, namely that this "leading" oscillation is utterly insignificant for small values of Z. One has to be at enormous Z, i.e., really far in the asymptotic domain, to see this contribution actually dominate the rest. To be more specific, we display the amplitudes of the individual terms numerically; they are given by

$$-\frac{(-1)^m}{j^{3/2}}\frac{0.006\,816Z^{1/6}}{1.127j^2-m^2}Z^{4/3} = Z^{4/3}\times\begin{cases}0.000\,687Z^{1/6} & \text{for } j=2,\ m=1\,,\\ (-0.000\,214Z^{1/6}) & \text{for } j=3,\ m=2\,,\\ 0.000\,144Z^{1/6} & \text{for } j=3,\ m=1\,,\\ \ldots.\end{cases} \tag{108}$$

[The numerical value of $\dot\nu''_0$ needed in (108) is computable from (100) in combination with $\nu_\varepsilon(0)=\lambda_\varepsilon\nu'_\varepsilon-\frac{1}{2}\lambda_\varepsilon^2\nu''_\varepsilon$.] Inasmuch as $Z^{1/6}$ is at most 2.24 in the range of interest, the amplitude of the λ,ν binding-energy oscillation is indeed negligible. For it to be of the size of the λ oscillation of Fig. 8, one needs[19] $Z^{1/6}\cong 90$, i.e., $Z\cong 5\times 10^{11}$—far beyond the domain of physics.

DISCUSSION

The time has come to put things together. Since both the ν and the λ,ν oscillations are negligible, our semiclassical prediction for the binding-energy oscillations consists of the leading and the next-to-leading λ oscillations of Eqs. (82)—(84), of which partial sums are plotted in Figs. 8 and 10. Their sum is now compared to the HF prediction in Fig. 12.

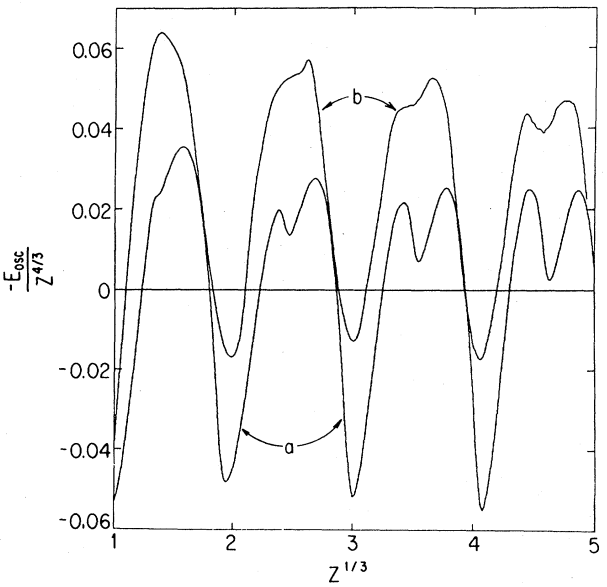

FIG. 12. Comparison of our semiclassical prediction for the nonrelativistic binding-energy oscillations (curve *a*) with the HF prediction (curve *b*).

Both curves agree in a number of details. First, they have the same phase and period, which, as we have learned, is given by λ_0, the maximum value of the angular quantum number in the TF limit. Then their amplitudes are about the same. Further, they both show rather sharp structureless minima, while the maxima possess an evolving double structure.

There are two major differences between the HF curve and the semiclassical one. The less serious one is that the semiclassical curve is shifted down by what looks like a constant in Fig. 12. The reason thereof is that our calculation picked out only the oscillatory contributions of $E_{\rm qu}$—smooth terms have been consistently disregarded. Incidentally, adding terms to the semiclassical binding energy, such as $aZ^{4/3}+bZ^{3/3}$, that shift curve a of Fig. 12 up may also slightly relocate its extrema to the further benefit of the comparison with the HF curve. The second difference between the two curves is the more pronounced double structure of the semiclassical maxima. Inasmuch as they are produced by the interference of the leading and the next-to-leading λ oscillations, which have maxima at different values of $Z^{1/3}$, it is possible that matters change when Eq. (82) is improved by the inclusion of terms with amplitudes proportional to $Z^{-2/3}, \ldots$. Such higher-order oscillations could well effectively modify the leading oscillations so that they acquire small, $Z^{1/3}$-dependent, phase shifts. We have seen such phase shifts in II when studying Coulombic degeneracy [recall the remark made about $\langle y \rangle$ after Eq. (16) of II]. In short, the quantitative aspects of the double structure are likely to change slightly as soon as further oscillatory contributions are included. Also, up to now, the experimentally available data do not tell us what these binding-energy oscillations look like in detail in the real world.

One could wonder how a different choice of ν_0'' would have affected the final outcome. It is clear from Eqs. (83) and (84) that smaller values of ν_0'' move us closer to the asymptotic region, while a larger ν_0'' causes the sums over the various $\tilde{f}(z_0)$, etc., to constitute a larger correction of the asymptotic s_k and c_k. Consequently, the smaller the ν_0'' the more we see of the asymptotic half-period structure. This is illustrated in Fig. 13, where the semiclassical prediction is plotted for nine different multiples of our first-choice ν_0'', covering the range from $0.6\nu_0''$ to $1.4\nu_0''$. Although the largest of all these values is more than twice as big as the smallest one, the curves do not change dramatically. They all have the same overall appearance, the main difference being in the size of the double structure of the maxima. Therefore, we see no reason for arbitrarily revising our selection of ν_0''.

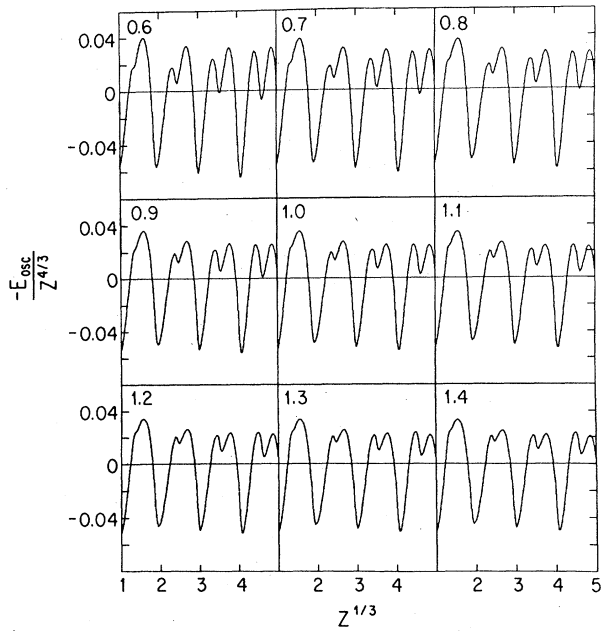

FIG. 13. Dependence of the semiclassical binding-energy oscillation on the choice for ν_0''. Plots are for ν_0'' equaling 0.6, 0.7, . . . , 1.4 times $\nu_0''=(\nu_0'-1)/\lambda_0=1.01044/Z^{1/3}$.

As we have remarked earlier [after Eq. (40)], the chosen approximation for $\nu_\varepsilon(\lambda)$ is such that it does not reproduce the correct value of $N_{\rm TF}(\varepsilon=0)$, namely Z. Instead, it gives only 91% thereof. This, however, does not discredit our approximate $\nu_\varepsilon(\lambda)$, because its job was *not* to mimic the smooth part of $N_{\rm qu}(\varepsilon)$ and $E_{\rm qu}$, but to yield the oscillatory terms correctly. And for those, $N_{\rm TF}(\varepsilon)$ is unimportant, whereas the slopes of $\nu_\varepsilon(\lambda)$ at $\lambda=0$ and λ_ε are of crucial influence. It is rather difficult to obtain the smooth $E_{\rm stat}$ of (1) by employing an approximation for $\nu_\varepsilon(\lambda)$, because the dependence on ε has to be correctly represented for a very large range of ε. Indeed, $E_{\rm stat}$ has been derived with different methods. On the other hand, the binding-energy oscillations stem from the electrons filled in last, which is to say from the range of ε close to $\varepsilon=0$. There, such an approximation for $\nu_\varepsilon(\lambda)$ is justifiable, and, as we have seen, works just fine.

Our approximate $\nu_\varepsilon(\lambda)$ is such that close to $\lambda=\lambda_\varepsilon$ it agrees with the TF line of degeneracy, while it deviates considerably for $\lambda\cong 0$. Why have we been so concerned with one end of the line and not with the other? The reason is that the shape of $\nu_\varepsilon(\lambda)$ near $\lambda=\lambda_\varepsilon$ is determined by the potential around $r=r_\varepsilon$, i.e., in the dense interior of the atom. Here the TF potential is very realistic for sufficiently large Z. In contrast, when $\lambda\cong 0$ and $\varepsilon\lesssim 0$, the value of $\nu_\varepsilon(\lambda)$ is to a great extent related to the potential at far distances. There the TF potential is seriously in error, as it falls off much too slowly. In other words, for $\lambda\cong\lambda_\varepsilon$ the TF lines of degeneracy are trustworthy, whereas they are not for $\lambda\cong 0$ when $\varepsilon\lesssim 0$. Therefore, any special effort, aiming at an accurate agreement between the approximation for $\nu_\varepsilon(\lambda)$ and the exact TF line of degeneracy, is not called for beyond the region of $\lambda\cong\nu_\varepsilon$. Please observe that, consistent with these remarks, all parameters—such as λ_0, ν_0', $\dot{\lambda}_0$, $\dot{\nu}_0'$, $\ddot{\lambda}_0$, and also ν_0''—entering the final result of the semiclassical calculation are entirely given by the potential and its derivatives at $r=r_0$.

CONCLUDING REMARKS

We labored mightily to produce a semiclassical result that is not essentially different from the previously known HF prediction. Why did we choose to do so? Because now we have an understanding of the physical origin of the nonrelativistic binding-energy oscillations. Although

the HF method produces the curve of Fig. 2 [strictly speaking, not even that, since E_{stat} of (1) is not a HF result], it provides no insight whatsoever for the origin of these oscillations.

The HF method is designed for the investigation of individual atoms with given nuclear charge and number of electrons. In contrast, the semiclassical approach is meant to deal as a whole with the Periodic Table. It is therefore capable of producing E_{stat} of (1) and also of illuminating E_{osc}: It has told us that the period of the oscillations is directly related to the largest angular quantum number, that the amplitude is proportional to $Z^{4/3}$, and how the double structure of the maxima comes about. This remarkable achievement of the semiclassical method demonstrates that it is sufficiently refined to describe atomic properties that are attributable not only to the central bulk of electrons, but also to the relatively few outer electrons. This points to possible future applications. For example, the calculation of atomic electric polarizabilities requires a good description of the loosely bound electrons at the edge of the atom. So far, it has been notoriously difficult to handle these electrons with sufficient accuracy in TF-type statistical models, although certain improvements have already been made.[20] The new semiclassical method is likely to take the next step in this direction.

ACKNOWLEDGMENTS

We would like to thank Dean Harold Ticho and Dean Clarence Hall, as well as the Office of Academic Computing at the University of California at Los Angeles for making computer time available to us. One of us (B.-G.E.) gratefully acknowledges the generous support by the Alexander von Humboldt Foundation.

---

[1]The first term is the TF energy; see, for example, P. Gombás, *Die statistische Theorie des Atoms und ihre Anwendungen* (Springer, Vienna, 1949).

[2]The second term is the correction for strongly bound electrons; see J. M. C. Scott, Philos. Mag. **43**, 859 (1952); J. Schwinger, Phys. Rev. A **22**, 1827 (1980).

[3]The third term is due to exchange (accounts for $\frac{9}{11}$) and quantum corrections to the kinetic energy (remaining $\frac{2}{11}$); see J. M. C. Scott, Ref. 2; J. Schwinger, Phys. Rev. A **24**, 2353 (1981).

[4]J. P. Desclaux, At. Data Nucl. Data Tables **12**, 311 (1973).

[5]This kind of plot was first given by I. K. Dmitrieva and G. I. Plindov, J. Phys. (Paris) **43**, 1599 (1982).

[6]In doing so, we honor a promise that we gave in B.-G. Englert and J. Schwinger, Phys. Rev. A **29**, 2339 (1984).

[7]B.-G. Englert and J. Schwinger, this issue, Phys. Rev. A **32**, 26 (1985).

[8]B.-G. Englert and J. Schwinger, preceding paper, Phys. Rev. A **32**, 36 (1985).

[9]C. E. Moore, *Atomic Energy Levels,* Natl. Bur. Stand. Ref. Data Ser., Natl. Bur. Stand. (U.S.) Circ. No. **35** (U.S. GPO, Washington, D.C., 1970).

[10]J. Schwinger, Ref. 2; I. K. Dmitrieva and G. I. Plindov, Ref. 5.

[11]J. M. C. Scott, Ref. 2.

[12]S. Fraga, J. Karowowski, and K. Saxena, *Handbook of Atomic Data* (Elsevier, Amsterdam, 1976). The correction in question is, for calcium, 365 cm^{-1} out of a total binding energy of 1.49×10^{8} cm^{-1}.

[13]This gives the leading term of E_{stat} in (1), of course.

[14]H. Hellmann, Acta Physicochim. URSS **4**, 225 (1936), was the first to consider the *l*TF model. He did not, however, use the Fourier formulation but the original sum over l. Therefore, he failed to recognize that E can be split into E_{TF} plus the quantum correction E_{qu}.

[15]Recreation of the original sum over l by employing the Poisson identity [Eq. (26) of I] would turn Eqs. (17) and (5) together into the energy functional obtained quite differently by Hellmann.

[16]A standard reference is M. Abramowitz, in *Handbook of Mathematical Functions,* edited by M. Abramowitz and I. Stegun (Dover, New York, 1972).

[17]Equation (47) happens to be also true for the Tietz potential (see II).

[18]For reference, see W. Gautschi, in *Handbook of Mathematical Functions,* edited by M. Abramowitz and I. Stegun (Dover, New York, 1972).

[19]This makes use of the observation that $s_2-s_{-2}\cong0.06$ for large Z, so that there the leading λ oscillation has an amplitude of about $0.06Z^{4/3}$.

[20]B.-G. Englert and J. Schwinger, Ref. 6.